Supplementary Supporting Information

Enhancement in intramolecular interactions and *in vitro* biological activity of a tripodal tetradentate system upon complexation

Nidhi Tyagi,[a] Mambattakkara Viji,[a] Suneesh C. Karunakaran,[a] Sunil Varughese,[a] Shilpa Ganesan,[b] Sulochana Priya,[b] P. S. Saneesh Babu,[c] Asha S. Nair,[c] and Danaboyina Ramaiah[a,d*]

[a]*Photosciences and Photonics, Chemical Sciences and Technology Division,* [b]*Agroprocessing and Natural Products, CSIR-National Institute for Interdisciplinary Science and Technology (CSIR-NIIST), Thiruvananthapuram 695019, India.* [c]*Cancer Research Program, Rajiv Gandhi Centre for Biotechnology, Thiruvananthapuram - 695014, Kerala, India.* [d]*CSIR-North East Institute of Science and Technology (CSIR-NEIST), Jorhat - 785006, Assam, India.*

*To whom correspondence should be addressed at: Tel +91 376 2370012; Fax +91 376 2370011; E–mail: rama@rrljorhat.res.in and d.ramaiah@gmail.com

1. Experimental Section

1.1. Materials and Methods

The melting points were determined on a Mel-Temp II melting point apparatus. ^{1}H and ^{13}C NMR were recorded on a 500 MHz Bruker advanced DPX spectrometer. IR spectra were recorded on a Perkin Elmer Model 882 infrared spectrometer with KBr disks in the range 4000–400 cm^{-1}. MALDI-TOF MS analysis was performed with a Shimadzu Biotech Axima CFR plus instrument equipped with a nitrogen laser in the linear mode. The electronic absorption spectra and fluorescence spectra were recorded on a Shimadzu UV-VIS-NIR scanning spectrophotometer and SPEX-Fluorolog F112X spectrofluorimeter. Quantum yields of fluorescence were measured by equation 1 using optically dilute solutions (quinine sulphate solution is used as standard). Fluorescence lifetimes were measured using IBH picoseconds time correlated single photon counting system. The fluorescence decay profiles were deconvoluted using IBH data station software V2.1 and minimizing the χ^2 values of the fit to 1± 0.1. Magnetic susceptibilities were determined at 296 K with Vibrating Sample Magnetometer model 155, using nickel as a standard. Soution state magnetic moment were determined at room temperature using the Evans method. Diamagnetic corrections were carried out with Pascal's increments.[1] Molar conductivities were determined in DMF at 10^{-3} M at 25 ^{0}C with a Systronics 304 conductometer. Cyclic voltammetry measurements were carried out using a CV-50W elctroanalyzer in DMF using platinum wire as auxiliary electrode, glassy-carbon as working electrode. The potentials were referenced to the standard Ag/AgCl electrode and ferrocene (0.53 V, $E_{1/2}$) was used as an internal standard.

All the solvents were dried prior to use. Anhydrous $FeCl_3$ and $Cu(ClO_4)_2.6H_2O$ were purchased from Aldrich and S. D. Fine Chemicals, India and used without further purification. Tris(2-benzimidazolylmethyl)amine, (m.p. 277–281 °C) and 2-(3-bromo-propyl)-benzo[de]isoquinoline-1,3-dione (m.p. 138–140 °C) was prepared by reported procedures.[2] Calf thymus DNA (CT-DNA), BSA, ethidium bromide (EB) and oligonucleotides (**DNA1**; 5′ CAC TGG CTT TTC GGT GCAT, **DNA2**: 5′ ATG CAC CGA AAA GCC AGTG were purchased from Sigma.

1.2. X-ray Crystallography

Single crystals of **Bz-NI**·$3H_2O$ and **2**·2DMF·$4H_2O$ were obtained from a CH_2Cl_2–CH_3OH mixture and DMF, respectively. The data sets for the single-crystal X-ray studies for **Bz-NI**·$3H_2O$ and **2**·2DMF·$4H_2O$ were collected with Mo Kα (λ = 0.71073 Å) radiation on a RIGAKU diffractometer. All the calculations were performed using SHELXTL.

1.3. DNA Binding Experiments

The DNA binding experiments were performed in 10 mM phosphate buffer (pH 7.4) (2 mM NaCl) using DMF-buffer (15%) solution. A solution of calf thymus DNA (CT-DNA) was sonicated for 2 h and filtered through a 0.45 μM millipore filter. The concentration of CT-DNA was determined from the absorption intensity at 260 nm with ε value of 6600 $M^{-1}cm^{-1}$.[3] Absorption titration experiments were made using different concentration of CT-DNA, while keeping the complex concentration constant. Samples were equilibrated at room temperature for 5 min before recording each spectrum. Fluorescence emission spectra of the DNA–EB system were determined with DNA pre-treated with ethidium bromide (EB) at a ratio of [DNA]/[EB] = 2 for 30 min in 15% DMF-H_2O. Subsequently, varying concentrations of **1** and **2** (0-10 μM) were gradually dispensed into the cuvette, incubated for 5 min at room temperature. The fluorescence emission spectra of the samples were recorded from 530 to 800 nm by using λ_{ex} at 510 nm. DNA melting experiments were carried out by monitoring the absorption intensity of oligonucleotides (**DNA1**: 5′ CGT GCA TGC ACG GTAC-3′, **DNA2**: 5′ GTA CCG TGC AAT GTC CACG-3′) (2 μM) at 260 nm at various temperatures, both in the absence and presence of **1** and **2** (2-5 μM). ΔT_m values were calculated by determining the midpoints of melting curves from the first-order derivatives. Viscometric titrations were performed using LAUDA DLK10 automated viscometer, thermostatted at 25 °C in a constant temperature bath. The concentration of CT DNA was 100 μM, and the flow times were measured with an automated timer. Each sample was measured 3 times and an average flow

time was calculated. Data were presented as $(\eta/\eta_0)^{1/3}$ versus [complex]/[DNA], (η, η_0: Specific viscosities of DNA in presence and absence of complexes respectively).[4]

1.4. Protein Binding Studies

Spectrofluorimetric titrations of **1** and **2** (0-16 μM) in DMF-buffer (15%) solution at pH 7.4 (λ_{ex} = 345 nm) was also performed with increasing concentration of BSA. Quenching of the fluorescence emission of tryptophan residues of BSA was done using **1** and **2** as quenchers. To solutions of BSA in phosphate buffer at pH 7.4, increments of quenchers were added and the emission signals at ~344 nm (λ_{ex} at 280 nm) were recorded after each addition of the quenchers at the corresponding temperature (27 ^{o}C and 37 ^{o}C). Conformational changes were studied using synchronous fluorescence measurements. Synchronous fluorescence spectral studies were performed at $\Delta\lambda$ = 15 nm and 60 nm using similar concentration of BSA.

1.5. Cytotoxicity Studies Using MTT Assay

MTT assay was done to measure the effect of ligand and metal complexes on the growth inhibition of human cervical cancer (HeLa) cells and H9c2 cell lines.[5] Cells were treated with different concentrations of ligand and complexes for 24 h and the percentage of growth inhibition was calculated as follows,

% of growth inhibition = [1-absorbance of treated cells/absorbance of untreated cells] x100

1.6. Morphological analysis.

The morphological alterations in confluent monolayers of HeLa cells treated with or without metal complexes for 24 h and observed the transmitted light images to see the morphological alterations. (Magnification-40X)

1.7. Acridine Orange/Ethidium Bromide (AO/EB) Staining.

HeLa cells were treated with or without metal complexes for 24 h were washed with PBS and trypsinised. 25 μl of cell suspension (1x104 cells/mL) were incubated with 1 μl of acridine orange/ethidium bromide (one part each of 100 μg /mL of acridine orange and 100 μg/mL of ethidium bromide in PBS) just prior to microscopy.[6] A 10 μl of gently mixed suspension was placed on a microscope slide covered with glass slips and examined under fluorescent microscope (BD) connected to a digital imaging system.

1.8. DAPI staning.

DAPI staining[7] was done to study the nuclear fragmentation $1x10^4$/mL HeLa cells in the exponential growing phase were treated with 20 μM and 50 μM concentrations of both iron and copper complexes for 24 h. After treatment, cells were stained with DAPI (10 μg/ml) for 10 min, washed with PBS twice and images were taken using a Live Cells Imager (BD pathway TM Bioimage System, BD Biosciences).

1.9. Flow Cytometric Annexin V Apoptotic Studies.

Approximately 10^6 HeLa cells were seeded on 100 mm dishes and incubated for 24 h at 37 °C under 5% CO2. Cells were incubated with 5 and 10 μM of complex **2** as well as with 15 and 30 μM of complex **1** for 24 h. In this experiment, 0.1% DMSO were taken as control. Cells were stained with FITC-labeled Annexin using Annexin V–FITC apoptosis detection kit Sigma Aldrich) according to the manufacturer's instruction, and a flow cytometric analysis was then carried out using FACS Aria (BD, USA).

1.10. Immunoblot Analysis.

Approximately 10^6 HeLa cells were seeded on 100 mm dishes and incubated for 24 h at 37 °C under 5% CO2. Cells were incubated with 5 and 10 μM of complex **2** as well as with 15 and 30 μM of complex **1** for 24 h. In this experiment 0.1% DMSO were taken as control. Cells were then lysed, and the total protein content was measured using Bradford's reagent. Then 75 mg of total protein was loaded for SDS–PAGE, and immunoblotting was carried out using PARP antibody (cell signaling), and horseradish peroxidase-conjugated secondary antibodies (Santa Cruz) were used, followed by detection using enhanced chemiluminescence (ECL) method.

1.11. Lipophilicity

To quantify the lipophilicity of the ligand and complexes, water-octanol partition coefficients (P) were measured using the shake-flask method.[9] The log P values of the free ligands were also calculated using the online program ALOGSP 2.1 available at the Virtual Computational Chemistry Laboratory.[9] The resulting and calculated log P values are reported in Table S5.

1.12. Equations Employed

The quantum yields of fluorescence were calculated using (quinine sulphate (Φ_f = 0.54) in 0.1 N H_2SO_4 as standard) the equation 1,

$$\phi_u = \frac{A_s F_u n_u^2}{A_u F_s n_s^2} \phi_s \quad (1)$$

wherein, A_s and A_u are the absorbance of standard and unknown, respectively. F_s and F_u are the areas of fluorescence peaks of the standard and unknown and n_s and n_u are the refractive indices of the solvents used for the standard and unknown, respectively. Φ_s and Φ_u are the fluorescence quantum yields of the standard and unknown compound.

The intrinsic binding constants (K_{DNA}) were calculated by using equation 2,[8]

$$[DNA]/(\varepsilon_a-\varepsilon_f) = [DNA]/(\varepsilon_b-\varepsilon_f)+1/K_{DNA}(\varepsilon_b-\varepsilon_f) \quad .....(2)$$

wherein, [DNA] is the concentration of CT-DNA in base pairs. The apparent absorption coefficient ε_a was obtained by calculating A_{obsd}/[complex]. The terms ε_f and ε_b correspond to the extinction coefficient of free (unbound) and fully bound complexes, respectively. A plot of $[DNA]/(\varepsilon_a-\varepsilon_f)$ *vs* [DNA] gives K_{DNA} as the ratio of slope $[1/(\varepsilon_b-\varepsilon_f)]$ to intercept $[1/K_{DNA}(\varepsilon_b-\varepsilon_f)]$.

When a small molecules bind to a DNA or protein to a set of equivalent sites, the number of sites n can be obtained from the following equation,[10]

$$\log \frac{(I_0-I)}{I} = \log K_b + n \log[Q] \quad .....(3)$$

wherein, $K_b = K_{b,DNA}$ and $K_{b,BSA}$ is the binding constant of the complex with DNA/BSA and n is the number of binding sites per DNA/BSA molecule and [Q] is the total concentration of the quencher. The number of binding sites (n) and binding constant K_b have been calculated from linear fitting plots of $\log(I_0-I)/I$ *vs* log[Q] at different temperatures (300, 310 K).

The quenching parameter can be analyzed according to the Stern-Volmer equation,[11]

$$Io/I = 1 + K_{SV}[Q] \quad .....(4)$$

wherein, I_0 and I are the fluorescence intensities of the CT DNA in the absence and presence of complexes, respectively. K_{SV} is the Stern–Volmer dynamic quenching constant and [Q] is the total concentration of the quencher. From Stren-Volmer plot of I_0/I versus [Q], the quenching constants (K_{SV}) were obtained from the slop.

The bimolecular quenching constant (k_q) was evaluated from $k_q = K_{sv}/\tau_0$; wherein K_{SV} and τ_0 are Stern–Volmer quenching constant and average life time ($\tau_0 = 10^{-8}$ s) of BSA in the absence of quencher.[12]

The values of ΔH and ΔS can be estimated from the following van't Hoff equation,

$$ln\, K_T = -\frac{\Delta H}{RT} + \frac{\Delta S}{R} \quad \text{.....(5)}$$

The free energy changes (ΔG) at different temperatures can be calculated from the following relationship;

$$\Delta G = \Delta H - T\Delta S = -\mathrm{RT}\ln K \quad \text{.....(6)}$$

2. References

1 R. L. Dutta and A. Syamal, Elements of Magnetochemistry second ed Affiliated East-West Press, New Delhi, 1993. p. 8.

2 S. U. Hossain, S. Sengupta and S. Bhattacharya, *Bioorg. Med. Chem.,* 2005, **13**, 5750.

3 M. E. Reichman, S. A. Rice, C. A. Thomas and P. Doty, *J. Am. Chem. Soc.,*1954, **76**, 3047.

4 G. Cohen and H. Eisenberg, *Biopolymers,* 1966, **4**, 429; D. A. Scudiero, R. H. Shoemaker, K. D. Paull, A. Monks, S. Tierney, T. H. Nofziger, M. J. Currens, D. Seniff and M. R. Boyd, *Cancer Res.,* 1988, **48**, 4827.

6 J. H. Zhang, J. Yu, W. X. Li and C. P. Cheng, *Chin. J. Physiol.,* 1998, **41**, 121.

7 F. A. Tanious, J. M. Veal, H. Buczak, L. S. Ratmeyer and W. D. Wilson, *Biochemistry,* 1992, **31**, 3103.

8 A. Wolf, G. H. Shimer and T. Meehan, *Biochemistry,* 1987, **26**, 6392.

9 M. M. Saric, A. Mornar, T. B. Crnjevic and I. Jasprica, *Croatica Chem. Acta,* 2004, **1-2***,* 367

10 E.; Gratton, N. Silva, G. Mei, N. Rosato, I. Savini and A. Finazzi-Agro, *Int. J. Quantum. Chem*.,1992, **42**, 1479.

11 M. Lee, A. L. Rhodes, M. D. Wyatt, S. Forrow and J. A. Hartley, *Biochemistry,* 1993, **32**, 4237.

12 A. Divsalar, M. J. Bagheri, A. A. Saboury, H. Mansoori-Torshizi and M. Amani, *J. Phys. Chem. B,* 2009, **113**, 14035.

A)

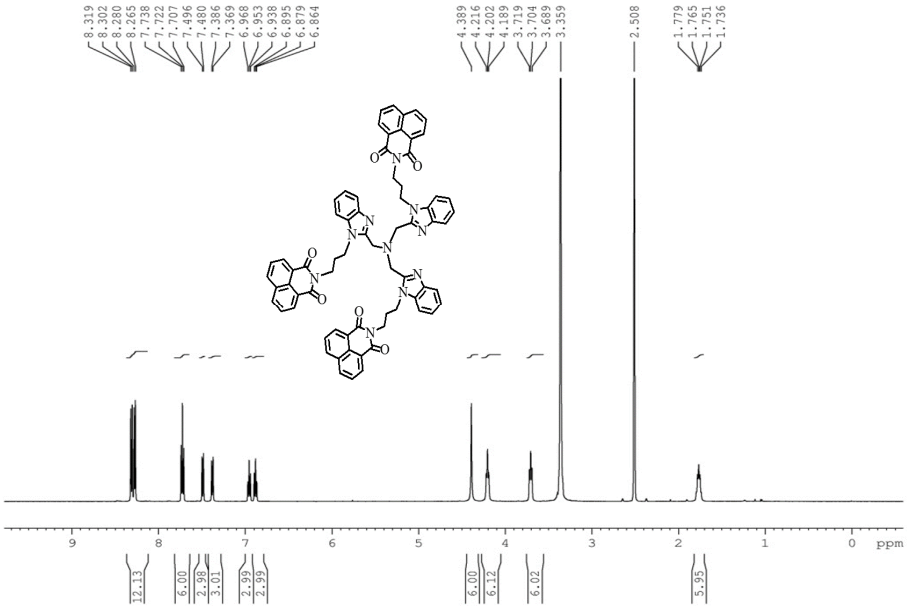
8.319
8.302
8.280
8.265
7.738
7.722
7.707
7.496
7.480
7.386
7.369
6.968
6.953
6.938
6.895
6.879
6.864
4.389
4.216
4.202
4.189
3.719
3.704
3.689
3.359
2.508
1.779
1.765
1.751
1.736
ppm
12.13
6.00
2.98
3.01
2.99
2.99
6.00
6.12
6.02
5.95

B)

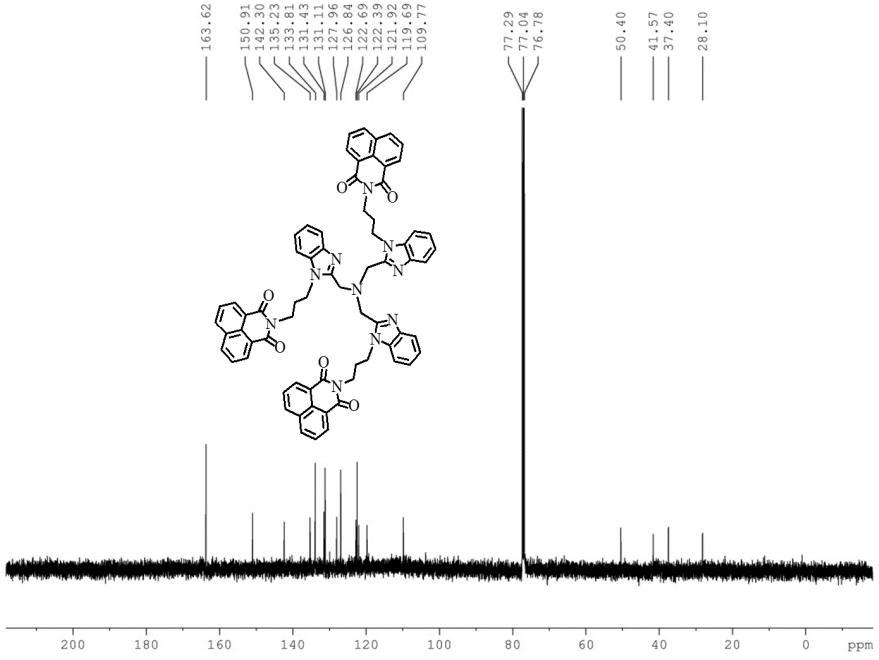
163.62
150.91
142.30
135.23
133.81
131.43
131.11
127.96
126.84
122.69
122.39
121.92
119.69
109.77
77.29
77.04
76.78
50.40
41.57
37.40
28.10
ppm

C)

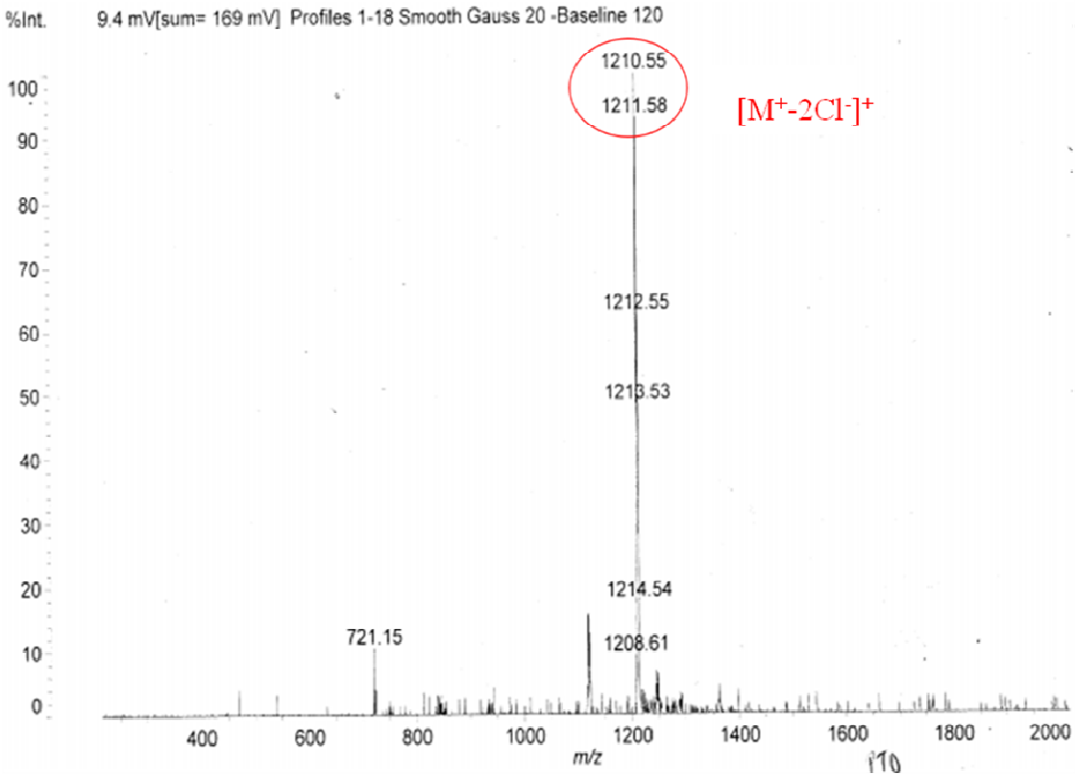

D)

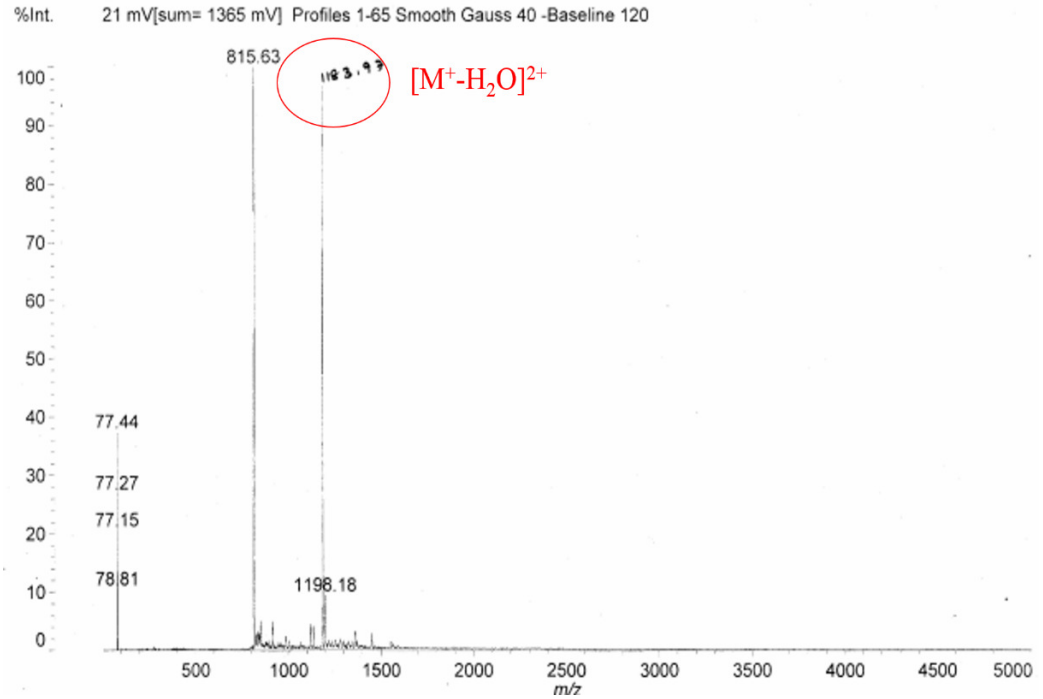

Fig. S1 A) ^{1}H NMR, B) ^{13}C NMR spectra of **Bz-NI** and MALDI-TOF mass spectrum of the complexes C) **1**, D) **2** in DMF.

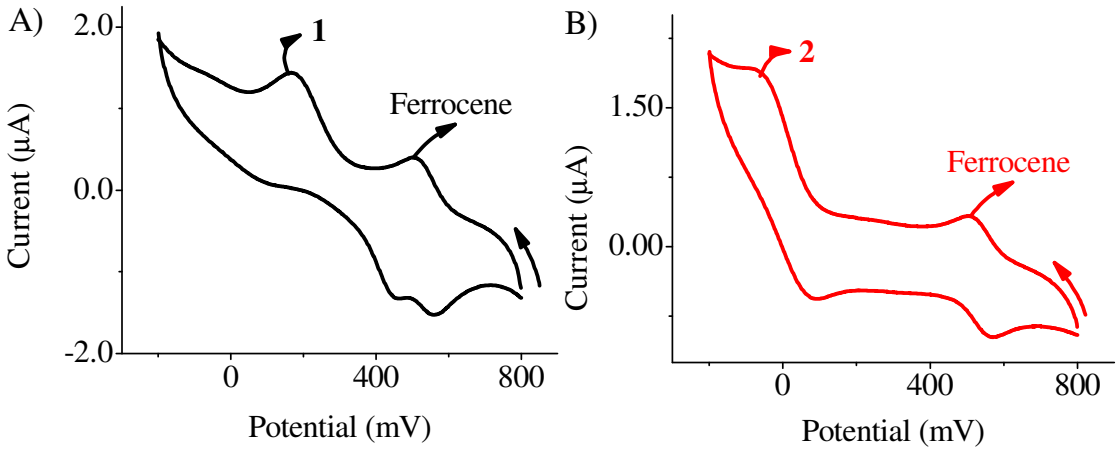

Fig. S2 Cyclic voltammogram of the complexes **1** and **2** (10^{-3} M) in DMF (scan rate 0.1 V/s) in presence of ferrocene (1 mM) as an internal standard.

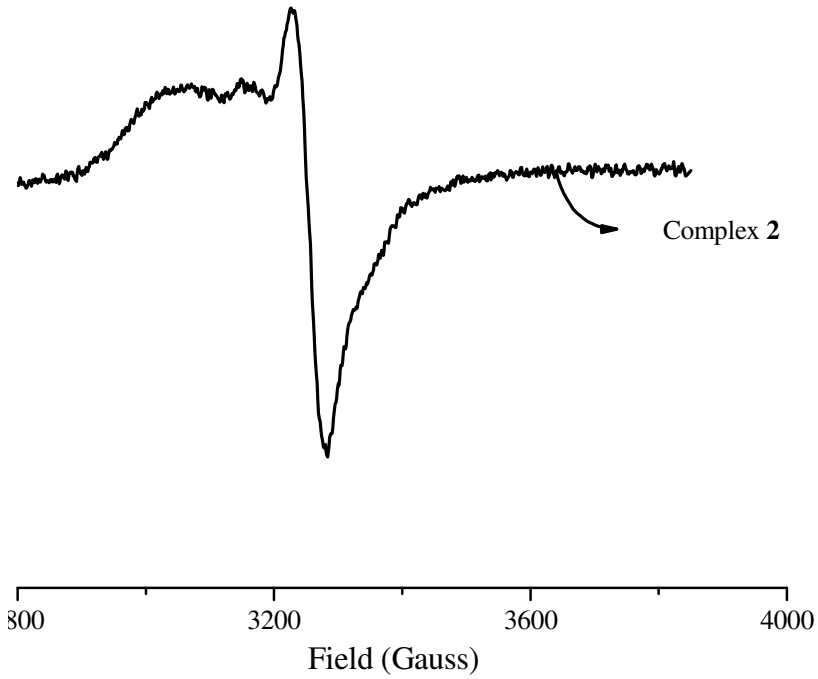

Fig. S3 X-band EPR spectrum of complex **2** in DMF solution at room temperature.

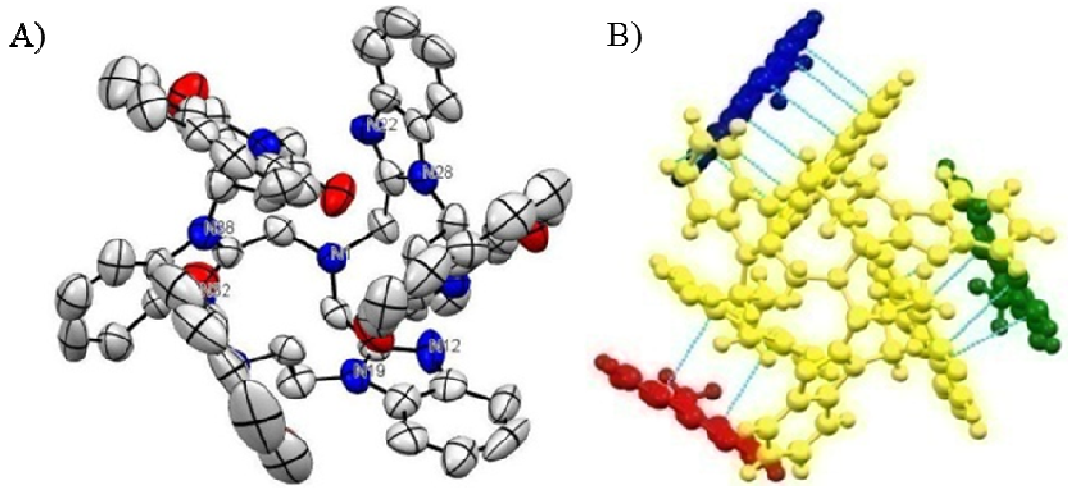

Fig. S4 ORTEP view of A) the ligand (**Bz-NI**) with ellipsoids at 50% probability level. (Solvent and hydrogen atoms have been omitted for clarity) B) Face-to-face stacking in **Bz-NI** exhibited by the naphthalimide moiety. Three distinct molecular units are represented as green, red and blue.

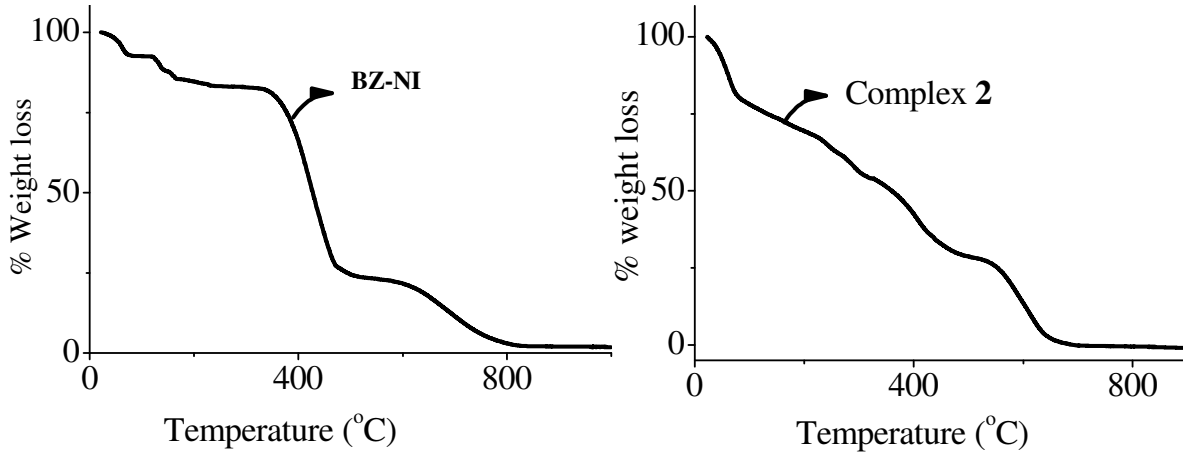

Fig. S5 TG analysis of the ligand (**Bz-NI**) and the complex **2**. (Based on the squeeze volume and electron count, the accounted electrons are 91 (i.e. 1 DMF and 2 water molecules) (for complex **2**). From the TG analysis we are getting a weight loss of ~20% by 90 °C. The calculated molecular mass of the structure (along with the unaccounted lattice solvents come to 1653) and the assumed weight loss of three DMF and eight water molecules (363) comes to ~21%, which is closely matching with the experimental value. TG for the ligand (**Bz-NI**) shows 11% weight loss by 90 °C (which accounts for a molecule of chloroform and methanol, with a calculated weight percentage of 11%) and by 150, another 5% which accounts for four water molecules. The calculated solvent molecules and the electron counts obtained from the SQUEEZE options are in agreement.)

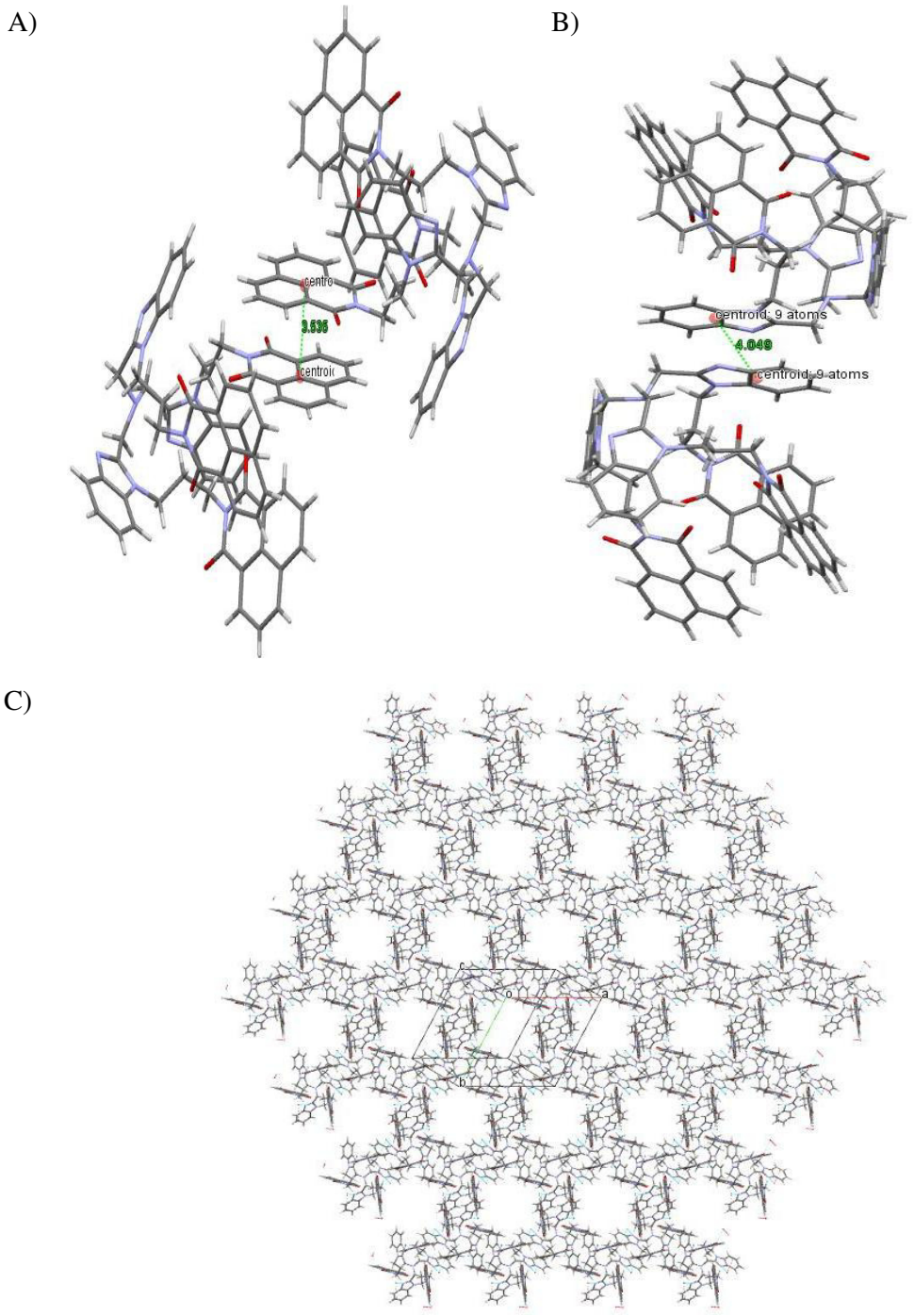

Fig. S6 Ligand showing intermolecular π-π stacking interaction between two neighbouring A) Naphthalimide B) Benzimidazolyl molecules and C) 3D network.

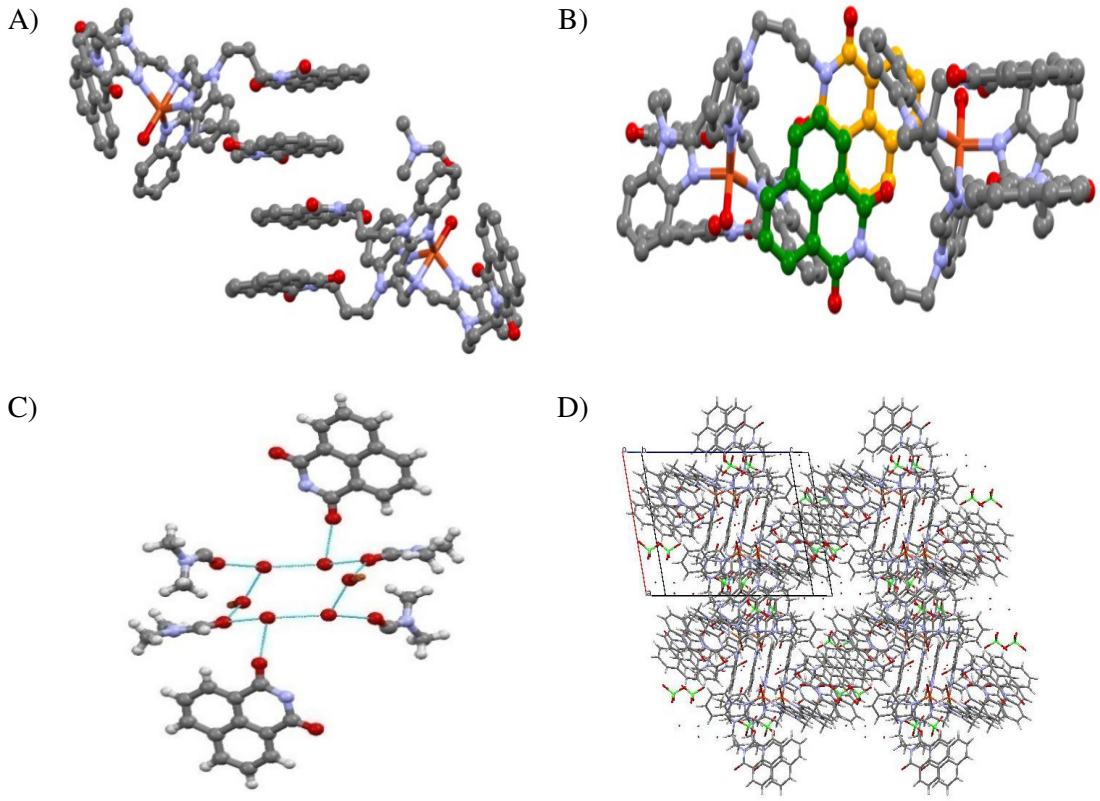

Fig. S7 A) Face-to-face stacking, B) Edge-to-edge stacking, C) The octamer hydrogen bonded network in the crystal, D) 3D network of Cu(II) complex along the b direction.

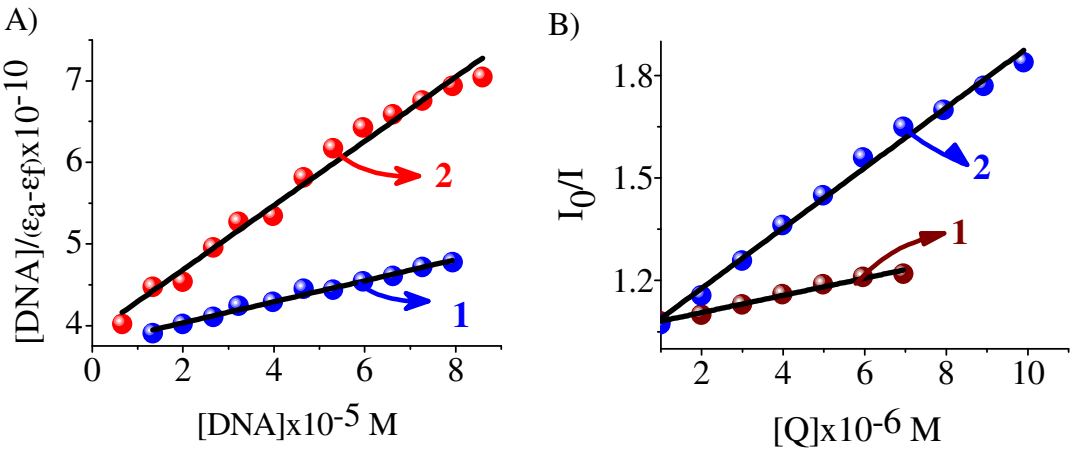

Fig. S8 A) The plot of $[DNA]/(\varepsilon_a-\varepsilon_f)$ *vs* [DNA] for the complexes **1** and **2**. B) The plot of I_0/I *vs* [Q] of the complexes **1** and **2**.

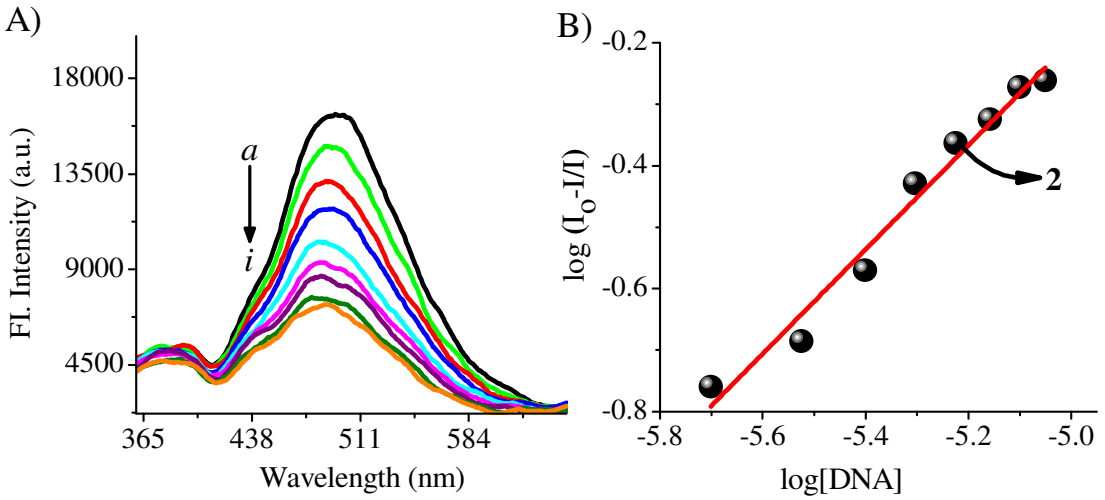

Fig. S9 A) Fluorescence emission spectra of **2** (10 μM) with increasing concentration of CT-DNA. [DNA]: a = 0; i = 8 μM; λ_{ex} = 345 nm, B) Double-log plots of the complex **2**.

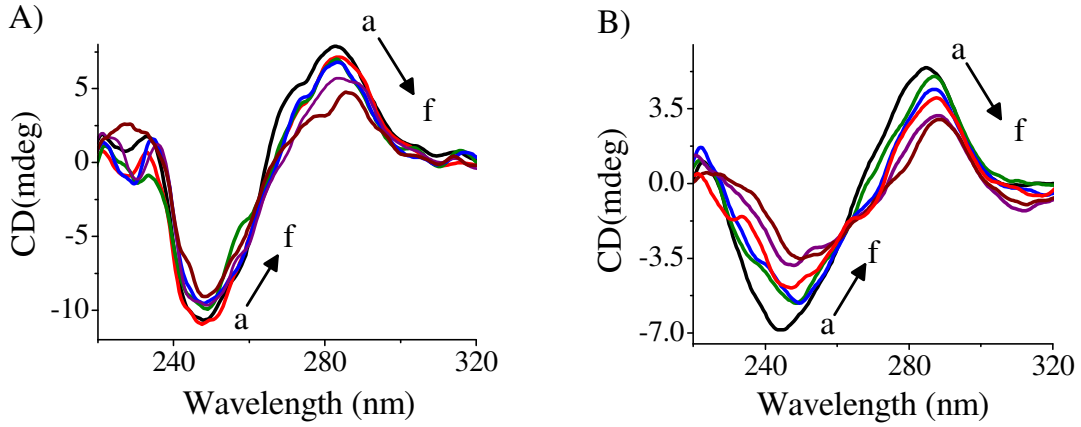

Fig. S10 Circular dichroism spectra of DNA in the absence and presence of complexes A) **1** and B) **2** in DMF phosphate buffer (pH 7.4). [Complex]: a = 0; f = 10 μM, [DNA] = 200 μM.

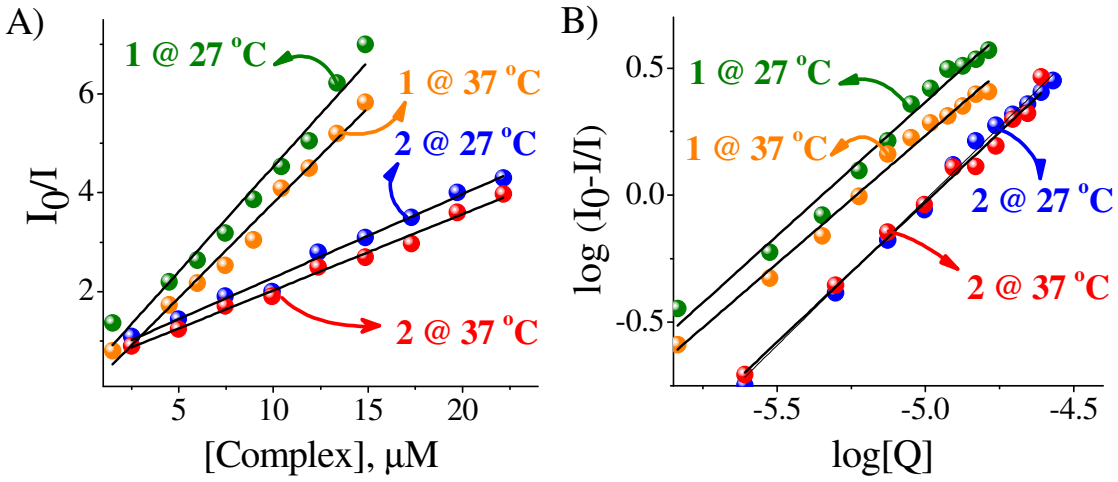

Fig. S11 A) Stern–Volmer curves of complexes **1** and **2** with BSA at 27 °C and 37 °C. B) Double-log plots of complexes **1** and **2** with BSA at 27 °C and 37 °C.

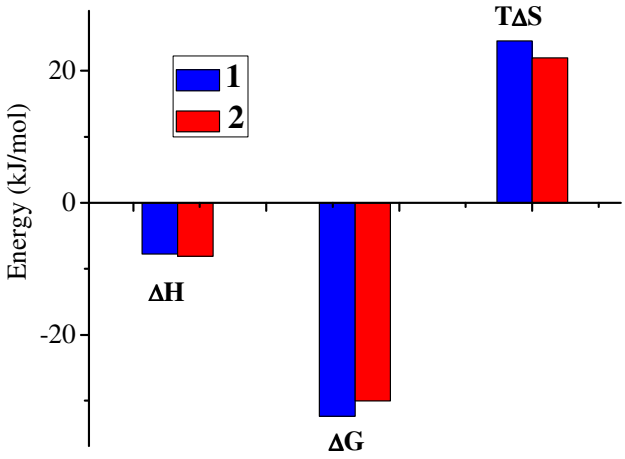

Fig. S12 Thermodynamic parameters of the interaction of BSA with **1** and **2**.

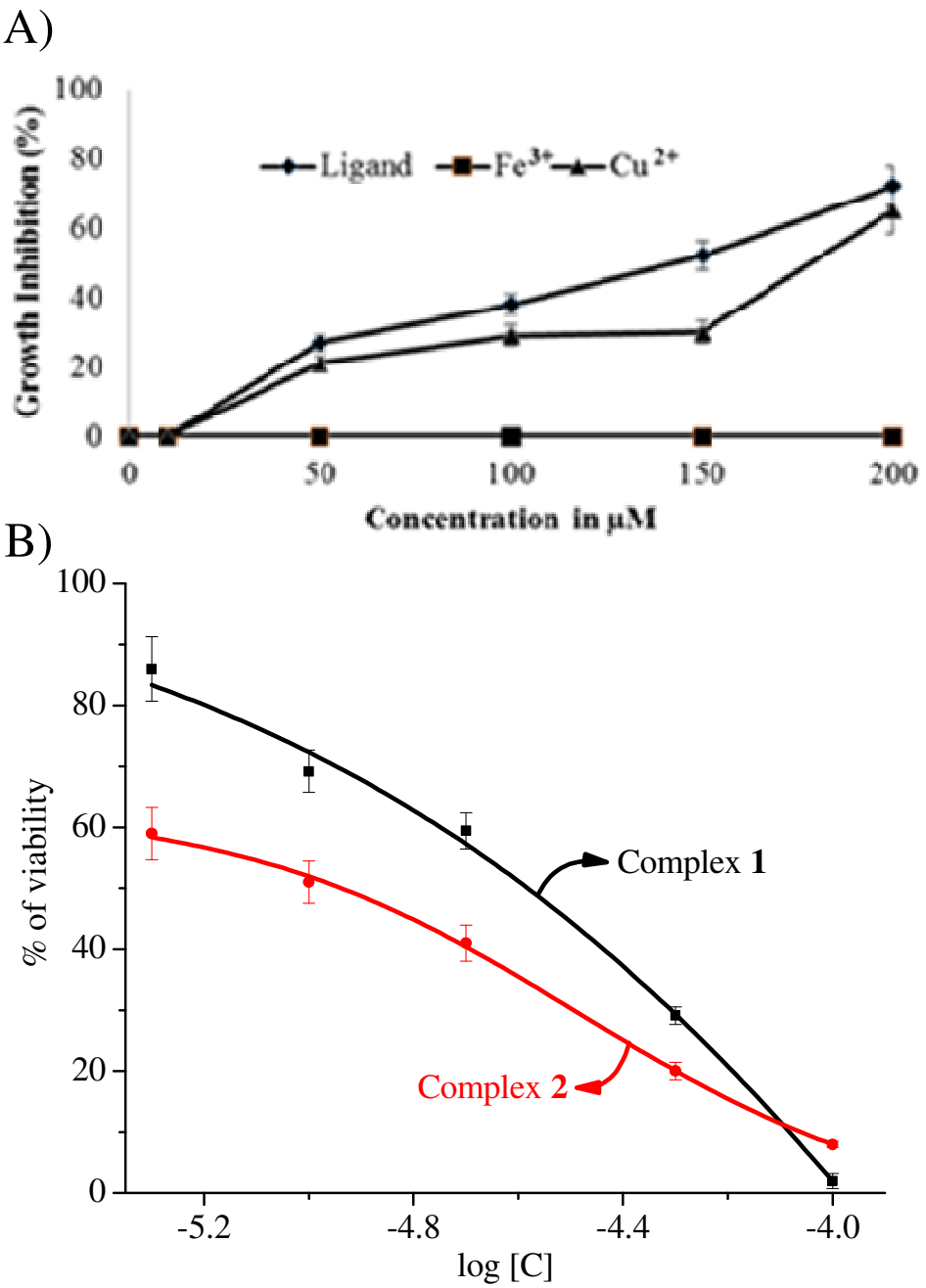

Fig. S13 A) *In vitro* cytotoxicity assay with different concentrations of the ligand (**Bz-NI**) and metal salts (0-200 µM) against the HeLa cell line. (Data are mean% ± SD of triplicate); B) Sigmoid fitted curves for the complexes **1** and **2** obtained by plotting cell viability against log[C] through ORIGIN 8.5 software.

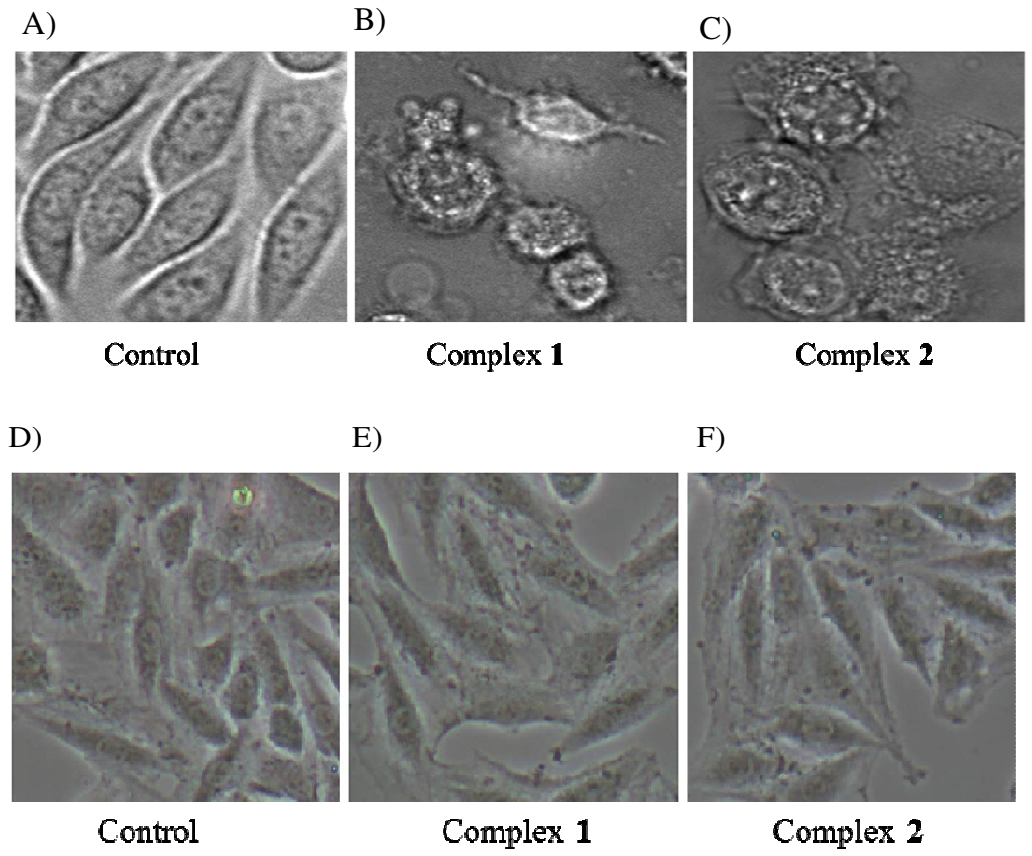

Fig. S14 Phase contrast images of A, D) control (*HeLa*) and (*H9C2*) cells; B-C, E-F) after treatment of the complexes **1** and **2** with *HeLa* and *H9C2* cell lines, respectively.

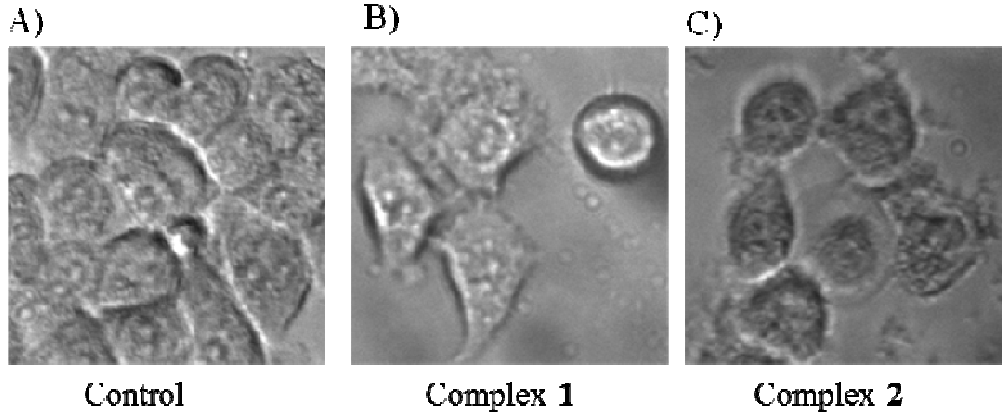

Fig. S15 Bright-field images of A) control (*HeLa*) cells B,C) complexes **1** and **2** respectively, after staining with DAPI.

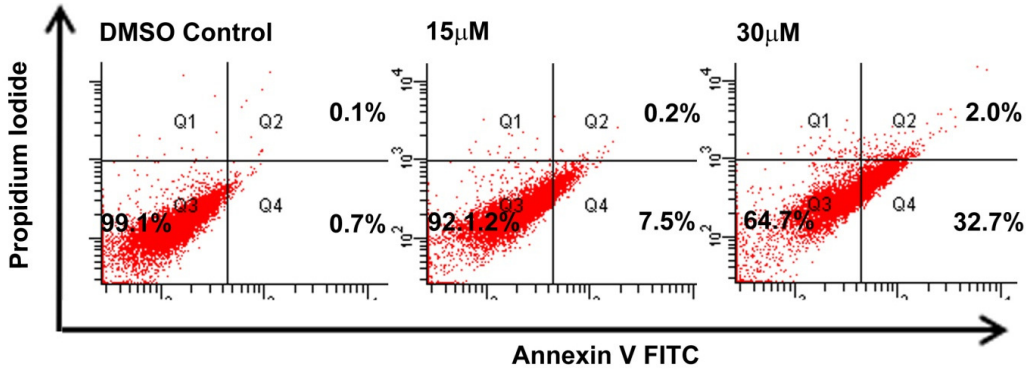

Fig. S16 Flow cytometric analysis of *HeLa* cells treated with different concentrations of the complex **1** for 24 h. The lower left quadrant of each panel shows viable cells, negative for Annexin V-FITC/PI. The lower right quadrants represent the apoptotic cells (annexin V-FITC+/PI-), while the upper right quadrants represent the necrotic or late-stage apoptotic cells (annexin V-FITC+/PI+).

Table S1. Cyclic voltammetric measurements[a]

Complexes	E_{pa}/mV	E_{pc}/mV	$E_{1/2}$[b], mV (ΔE_p[c], mV)	[d]$n=i_{Pa}/i_{Pc}$
1	450	172	311 (278)	0.9
2	95	-73	11 (168)	0.3

[a]Measured in DMF for **1**, **2** with 0.1 M tetrabutyl ammonium hexafluorophosphate. [b]$E_{1/2}$ is calculated as average of anodic (E_{pa}) and cathodic (E_{pc}) peak potentials $E_{1/2} = 1/2(E_{pa}+E_{pc})$; and [c]$\Delta E_p = E_{pa}-E_{pc}$ at scan rate 0.1 V/s. [d]Constant-potential coulometric data $n = i_{pa}/i_{pc}$ calculated for $1e^-$ transfer.

Table S2. Crystal data and structure refinement details for **Bz-NI**·$3H_2O$ and **2**·2DMF·$4H_2O$

	Bz-NI·$3H_2O$	**2**·2DMF·$4H_2O$
Formula weight ($gmol^{-1}$)	1171.25	1615.91
Crystal system	Triclinic	Triclinic
Space group	$P\bar{1}$	$P\bar{1}$
***a* (Å)**	15.68(2)	15.244(8)
***b* (Å)**	16.44(2)	15.370(9)
***c* (Å)**	17.69(2)	17.480(9)
α (°)	91.408(12)	82.582(8)
γ (°)	115.658(13)	80.483(19)
β (°)	117.999(12)	88.567(19)
***V* ($Å^3$)**	3477(9)	4005(4)
Z	2	2
Temperature /K	298(2)	123(2)
λ (Å) (Mo-K_α)	0.71073	0.71073
Crystal size (mm)	0.20x0.20x0.10	0.25x0.20x0.15
***F*(000)**	1228	1682
Theta range for data collection	2.998-26.250	3.001-26.247
Data/restraints/parameters	13667/0/799	15656/0/ 1025
GOF on F^2	0.707	1.024
R_1 [I > 2σ(I)]	0. 0886	0.0941
wR_2 [I > 2σ(I)]	0.2216	0.2206

Table S3. Selected bond lengths (Å) and bond angles (deg) for **Bz-NI**·$3H_2O$ and **2**·2DMF·$4H_2O$

S.No.	Bond Lengths (Å)		Bond Angles (deg)	
Bz-NI·$3H_2O$	N22-C22	1.322(7)	C32-C31-N1	111.9(4)
	N32-C32	1.334(7)	C12-C11-N1	110.9(4)
	N12-C12	1.320(6)	C22-C21-N1	111.6(4)
	N1-C11	1.482(7)		
2·2DMF·$4H_2O$	Cu1-N2	2.076(4)	O6-Cu1-N4	98.32(16)
	Cu1-N5	2.093(5)	O6-Cu1-N2	178.73(18)
	Cu1-N4	2.028(4)	O6-Cu1-N3	100.02(16)
	Cu1-N3	2.109(5)	O6-Cu1-N5	101.33(18)
	Cu1-O6	1.950(4)	N2-Cu1-N5	79.82(18)
			N2-Cu1-N3	80.06(16)
			N2-Cu1-N4	80.59(17)
			N5-Cu1-N3	109.11(17)
			N4-Cu1-N3	121.91(18)
			N4-Cu1-N5	120.35(17)

Table S4. Binding and relative thermodynamic parameters of BSA with complexes **1** and **2**

S.No.	Temp (K)	Binding constant K_b x 10^5 (M^{-1})	Number of binding site (n)	ΔH (kJ/mol)	ΔS (J/molK)	ΔG (kJ/mol)	R
1	300	4.1	1.05	-7.80	81.72	-32.31	0.981
	310	1.8	1.01			-33.13	0.988
2	300	5.0	1.14	-8.11	73.09	-30.03	0.995
	310	2.9	1.10			-30.76	0.989

[a]R is the linear correlated coefficient

Table S5. Experimentally measured and computed ligand log P values by ALOGSP 2.1 program.

Compound	Experimentally measured log *P*	Calculated ligand log *P*
Bz-NI	1.45	2.54
1	0.92	-
2	1.55	-